Ionic Liquids Curated by Machine Learning for Metal Extraction

Adroit T. N. Fajar, Aditya D. Hartono, Rahman Md Moshikur, and Masahiro Goto*

Read Online

ACCESS | Metrics & More | Article Recommendations | Supporting Information

ABSTRACT: Metals are key components of modern devices; however, available resources of these metals are limited. In this study, we used machine learning (ML) to curate ionic liquids (ILs) that are suitable for metal extraction. We proposed classification and regression models to unravel hidden patterns between IL structures and their specific properties, i.e., metal selectivity and eco-toxicity. Evaluations of ML models using cross-validation indicate that the models were reliable, as described by the accuracy score (0.82) and R^2 value (0.76). The models also revealed that the metal selectivity of ILs was determined by the cation and anion structures, and the eco-toxicity level was primarily affected by the cation structures. Guided by predictions from the trained models, we selected three ILs (out of the 150 IL structures we initially proposed) that have extraction selectivity toward platinum, lithium, and neodymium as well as low eco-toxicity. We then prepared the ILs in the laboratory and assessed their performance by standard solvent extraction. The experiments indicate that the recommended ILs from ML could selectively extract the targeted metals with high extraction efficiency (>80%), which demonstrates the feasibility of ML as a promising toolkit that can help accelerate innovations in metal extraction.

KEYWORDS: *classification, regression, random forest, platinum, lithium, neodymium*
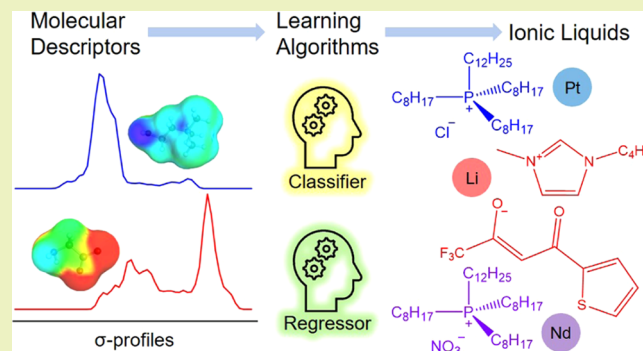
INTRODUCTION

Platinum group metals (PGM), metals in lithium-ion batteries, and rare-earth metals (REM) are essential components of modern devices. The demand for such critical minerals will continuously increase because they will play a crucial role in the ongoing clean energy transition.[1] However, most of these metals have limited availability.[2] Furthermore, current metal mining mainly relies on pyrometallurgical processes with high energy consumption from fossil fuels,[3] which indicates that increased metal production would increase carbon emissions into the atmosphere. Innovation in metal extraction that is economically feasible and eco-friendly is expected to address this issue. Several promising endeavors have been carried out in recent years (including the development of membrane separation,[4] aqueous biphasic systems,[5] solvometallurgy,[6] and bio-extractants[7]), despite the popularity of solvent extraction (i.e., liquid−liquid extraction) among practitioners in industry because of its practical implementation.

The efficiency of a solvent extraction depends on the performance of its extractant. Ionic liquids (ILs) could be excellent extractants because of their outstanding properties— such as negligible vapor pressure, presumably low toxicity, and vast tunability.[8] The latter is a useful feature for metal extraction because it is hypothetically possible to design a dedicated IL with high selectivity for extracting each metal on the periodic table. One can easily adjust the physical and chemical properties of an IL by varying the combination of its cation and anion, and in so doing induce countless permutations. Nevertheless, preparing ILs with specific properties is not always easy because syntheses can be costly and time-consuming. Furthermore, understanding the relationship between IL structures and their properties remains challenging.[9,10] One can estimate common physical properties such as melting point and solubility—using computational chemistry based on molecular dynamics simulations, density functional theory (DFT), or the conductor-like screening model for realistic solvents (COSMO−RS) theory.[11−13] However, unique features such as metal selectivity are extremely challenging to predict. Another attribute that would be useful in designing metal extractants is eco-toxicity. ILs are often assumed to have low toxicity, whereas recent reports indicate that the toxicity of ILs is not negligible and can vary in accordance with the structure.[14] Therefore, ILs with controllable selectivity toward critical metals and potentially having low eco-toxicity would be useful extractants for the metal mining and recycling industries.
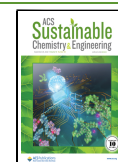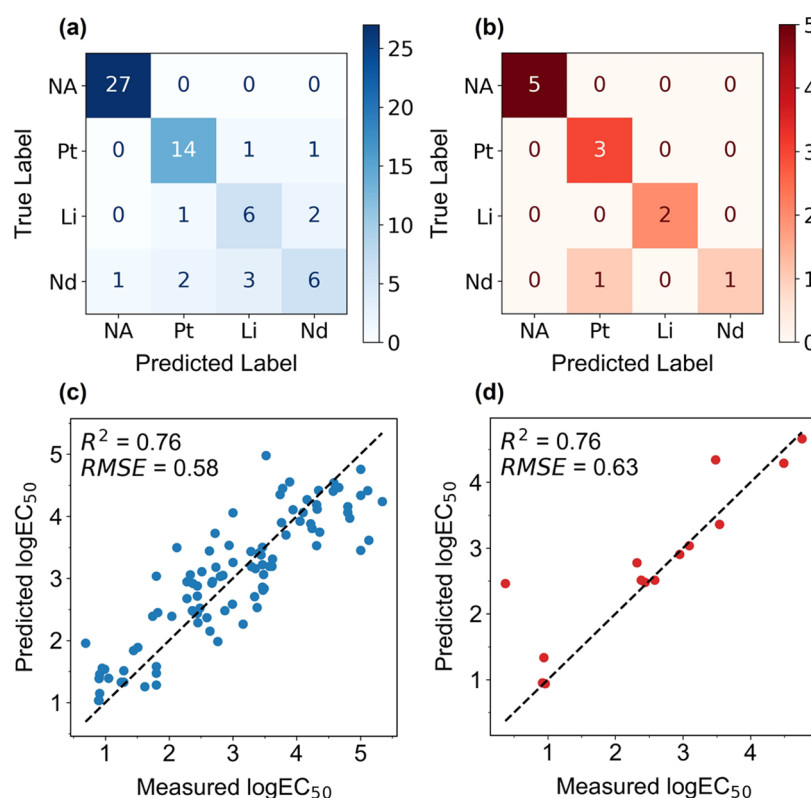
Figure 1. Confusion matrix plots of the predicted labels against true labels of the classification model evaluated by (a) cross-validation and (b) test dataset. Scatter plots of the measured $\log EC_{50}$ against the predicted $\log EC_{50}$ values of the regression model evaluated by (c) cross-validation and (d) test dataset.

In recent years, machine learning (ML) has been extensively reported as a promising tool for resolving problems in chemistry. Almeida et al. pointed out that chemists perceive intelligent machines as competitors; thus, these researchers helped to counteract such perceptions.[15] Similarly, we perceive ML to be a toolkit that compliments conventional computational chemistry approaches and thus accelerates innovations. Implementations of ML in chemistry research have been growing at an impressive rate lately.[16] This included the use of ML in comprehending zeolite synthesis,[17,18] predicting, e.g., metal−organic framework stability,[19] understanding organic reactivity,[20] and predicting the performance of batteries.[21] As such, using ML to address the challenge of predicting favorable characteristics of ILs as metal extractants would be advantageous.

Herein, we used ML to curate IL structures that have selectivity toward PGM, metals in lithium-ion batteries, and rare-earth metal representatives: platinum (Pt), lithium (Li), and neodymium (Nd), respectively. We selected the σ-profiles generated from DFT and COSMO−RS computations as the molecular descriptors of the IL structures. We prepared two ML models with the random forest algorithm: classification and regression models. We trained the classification model using a dataset of previously reported Pt(IV), Li(I), and Nd(III) extractions that used ILs. We assigned the regression model to capture the correlation between the IL structures and their eco-toxicity level. We then used the trained models to predict the metal selectivity and eco-toxicity of the 150 ILs we proposed. On the basis of the prediction results, we prepared ILs that are suitable for critical metal extraction in the laboratory. We then carried out selective extraction of Pt(IV),

Li(I), and Nd(III) using the ILs. To the best of our knowledge, the current work is the first to comprehensively investigate the implementation of ML to handle problems that are typically encountered in metal extraction.

■ RESULTS AND DISCUSSION

The ability of ML models to identify hidden patterns or fundamental relationships between chemical structures and particular properties is determined by the data quantity, molecular descriptor quality, and algorithmic complexity. This study used 186 data of IL structures to train the classification and regression algorithms, consisting of 76 data on metal selectivity and 110 data related to eco-toxicity levels. Generally, more training data would lead to better learning ability. Nonetheless, a smaller dataset with legitimate descriptors would lead to effective learning as well. We represented the molecular structures of the ILs by the σ-profiles generated by DFT and COSMO−RS calculations. A σ-profile gives the probability of finding a mean screening charge density on a specific contact segment of a molecule.[22] Several reports have demonstrated the capability of COSMO−RS approaches for investigating metal extraction behaviors.[23−26] In addition, the σ-profile is an excellent molecular descriptor for ML purposes.[27] Regarding the learning algorithm, we selected random forest for both classification and regression models. Random forest is an advanced ML algorithm that originates from the accumulation of its predecessor, the decision tree algorithm. As such, random forest offers exceptional learning capability for various types of data.[28]

We undertook the learning process by splitting the dataset into training and test data. We used the training data to
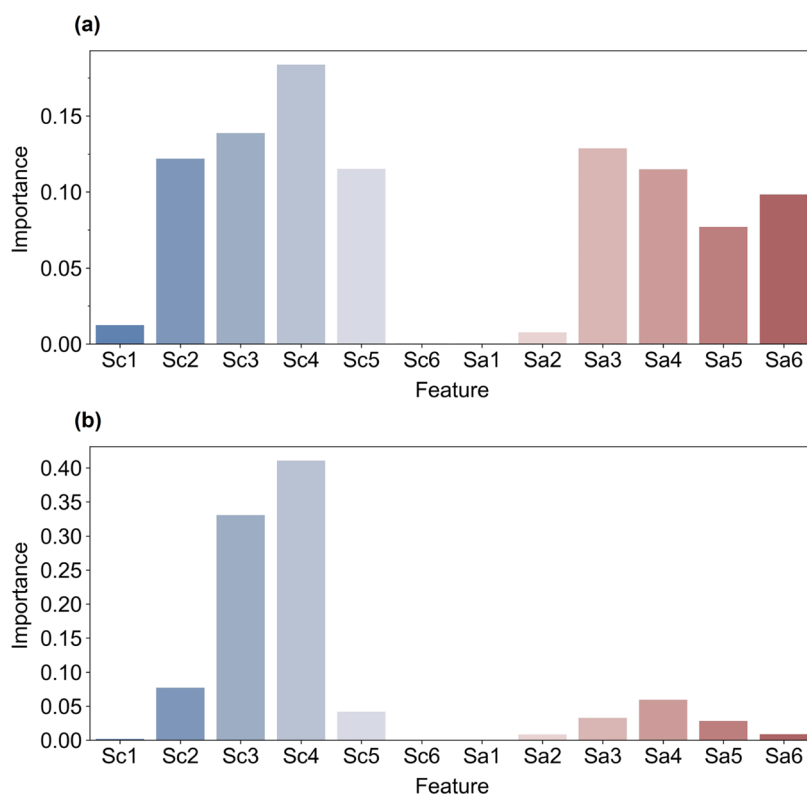
(a)

(b)

Figure 2. Importance of each feature within the descriptor on the (a) classification and (b) regression models.

construct and evaluate the ML models using cross-validation (Scheme S1, Supporting Information). We conducted cross-validation by executing the random forest algorithm multiple times across the training data, and thus generated various learning outcomes. We designated the average value of those outcomes as the characteristic performance of the models. Figure 1a shows the cross-validation behavior of the classification model. The model was correct 14× in predicting selectivity for Pt from 16 attempts, correct 6× in predicting selectivity for Li from nine attempts, and correct 6× in predicting selectivity for Nd from 12 attempts. Additionally, the model was always correct in predicting ILs that were not applicable (NA) for Pt, Li, and Nd extraction out of 27 attempts. The model had a total accuracy score of 0.82, which was relatively high considering that the value on cross-validation was the average of multiple iterations. We then tested the performance of the classification model in predicting the metal selectivity of the ILs on the test data (Figure 1b). The predictions for labels NA, Pt, and Li were always correct, whereas one prediction for Nd was false. The overall accuracy score on the test data was 0.91, which indicates a remarkably high performance. Figure 1c shows the cross-validation behavior of the regression model. The values of the measured $logEC_{50}$ against the predicted $logEC_{50}$ exhibited a linear correlation with an R^2 value of 0.76 and a root-mean-square error of 0.58, demonstrating that the model could recognize the correlations between the IL structures and their eco-toxicity. We obtained similar values of R^2 (0.76) and root mean square (0.63) on the test dataset (Figure 1d), indicating the model's reliability. In addition, we carried out a futile prediction on the training data without cross-validation, merely to confirm that the algorithms did learn from the prescribed data, which indicates perfect scores for both models (Figure

S1, Supporting Information). These results suggest that the ML models are reliable; thus, one can use them to predict the properties of new data.

Apart from its exceptional learning capability, the random forest algorithm offers additional functionality in revealing the importance of each considered feature within the descriptor. This ability is beneficial for the σ-profile descriptor because its features represent specific parts of a chemical structure. We described an IL structure by 12 features: six for the cation (Sc1−Sc6) and six for the anion (Sa1−Sa6); where S1 and S6 represent the highest positive and negative charge densities, respectively, of a molecule (Figure S2, Supporting Information). The scale of the σ-profile is from −0.03 to 0.03 e/Å^2; thus, dividing it into six parts can fairly capture specific portions of a molecule. Figure 2a indicates the important features that determine the metal selectivity of an IL based on the classification model. The essential features were distributed among Sc2−Sc5 and Sa3−Sa6. This observation indicates that both the cation and anion structures of an IL were equally crucial to its metal selectivity. The features Sc2−Sc5 represent the neutral and moderate charge density regions of a cation, which refers to the hydrocarbon chains and functional groups, respectively. Thus, although extraction mechanisms usually proceed via electrostatic interactions, steric effects from the hydrocarbon chain perhaps also had a substantial contribution. Furthermore, the feature Sc1 (the cation's highest charge density region) exhibited minimum importance. Regarding the anion, besides Sa3−Sa5, the feature Sa6 exhibited high importance as well, which indicates that an anion with high charge density, or a hard base in accordance with hard−soft acid−base theory, affects the metal selectivity. However, the algorithm considered Sc3 and Sc4 as the main important features that determine the $log\,EC_{50}$ values on the regression

model (Figure 2b). This analysis indicates that the eco-toxicity level of an IL was primarily affected by the structures of the cation, especially the hydrocarbon region. This finding is in agreement with traditional quantitative structure−activity relationship approaches that suggested a longer alkyl chain would exhibit higher toxicity than a shorter alkyl chain.[29,30] Understanding the importance of each feature within the molecular descriptor was extremely helpful in terms of guiding our design of ILs for metal extraction.

We proposed 150 IL structures that might be suitable for extraction of Pt(IV), Li(I), and Nd(III) (Table S1, Supporting Information). At this point, the ILs were not necessarily new or liquid at room temperature; instead, we systematically included a series of possible combinations of cations and anions. By doing so, we expected to discover some helpful insights from the prediction results and find a suitable IL for each targeted metal. We synergistically made the final decision regarding which ILs should be selected as the metal extractants between the ML suggestions and our considerations. The models provided recommendations on metal selectivity and eco-toxicity of the ILs, and we considered their, e.g., synthetic simplicity, stability, and hydrophobicity. We avoided selecting ILs with the following characteristics: (i) extremely difficult to synthesize, (ii) not liquid at room temperature, and (iii) completely miscible with aqueous phases.

Figure 3 (top) shows the predictions of the metal selectivity and $\log EC_{50}$ values of the proposed ILs. The number of ILs

Figure 3. Predictions of metal selectivity and $\log EC_{50}$ values of 150 proposed ILs for carrying out metal extractions (top) and COSMO-surface images (not to scale) of the ILs selected in this study (bottom). Number of ILs in each predicted label: NA = 57, Pt = 14, Li = 28, Nd = 51.

that the classification model predicted to be selective for extraction of Pt(IV), Li(I), and Nd(III) was 14, 28, and 51, respectively, whereas the model predicted 57 ILs as NA. The predicted $\log EC_{50}$ values were distributed broadly, and included values <2.0 and >4.5. To give a sense of the scale, the toxicity level in accordance with the $\log EC_{50}$ values might be ranked as follows: highly toxic (<1), slightly toxic (1−2), moderately toxic (2−3), and practically harmless (>3).[31] Surprisingly, the regression model predicted most ILs with $\log EC_{50}$ of >3 as NA. These ILs were mainly choline-based

and some imidazolium-based. We further scrutinized this finding by looking up the predicted $\log EC_{50}$ values from the learning data for classification and the predicted selectivity from the learning data for regression (Figure S3, Supporting Information). The majority of the ILs previously used for extraction of Pt(IV), Li(I), and Nd(III) exhibited $\log EC_{50}$ values of <3, whereas ILs classified as NA had $\log EC_{50}$ values of >3 (Figure S3a). This information reveals that to date, eco-toxicity levels were not the primary concern in the design of metal extractants. We primarily acquired data of ILs classified as NA from the pharmaceutical field, which has strict regulations on biocompatibility. However, the predicted selectivity of ILs with measured $\log EC_{50}$ values of >3 from the learning data for regression was distributed to labels NA, Pt, Li, and Nd (Figure S3b). These findings indicate that there was a trade-off between the applicability of ILs as metal extractants and their toxicity level, yet designing ILs for metal extraction with low eco-toxicity is quite possible.

The ILs that the classification model predicted to be capable of extracting Pt(IV) exhibited predicted $\log EC_{50}$ values between ca. 2−3.5 [Figure 3 (top)]. IL_81 (1-butyl-3-methylimidazolium chloride) and IL_82 (1-butyl-3-methyl-imidazolium bromide) had predicted $\log EC_{50}$ values of 3.46 and 3.32, respectively. Unfortunately, these ILs are solid and fully soluble in water at room temperature. Similarly, IL_111, IL_112, and IL_114 had predicted $\log EC_{50}$ values of >2.5, but they are not liquids at room temperature. The next highest predicted $\log EC_{50}$ value for Pt (1.98) was IL_51 (trioctyldo-decyl phosphonium chloride, $[P_{88812}][Cl]$). We previously designed this IL in our laboratory for PGM extraction from a spent automotive catalyst.[32] We intentionally included it in the prediction to investigate its eco-toxicity level, which turned out to be fairly good. Thus, we selected IL_51 for the extraction of Pt(IV). The ILs that the ML model predicted to be capable of extracting Li(I) mainly exhibited $\log EC_{50}$ values of ca. 2.5. The top three values were 3.01, 2.86, and 2.76, which correspond to IL_85 (1-butyl-3-methylimidazolium hydrogen phosphate), IL_84 (1-butyl-3-methylimidazolium sulfate), and IL_87 (1-butyl-3-methylimidazolium hydrogen theonyltrifluoroaceto-nate, $[Bmim][TTA]$). IL_85 and IL_84 are water-soluble and solid at room temperature; thus, we selected IL_87 for Li(I) extraction. The ILs that the model predicted to be suitable for Nd(III) extraction mainly exhibited predicted $\log EC_{50}$ of ca. 2. Some of them had predicted $\log EC_{50}$ values of >2.5; however, similarly to the previous classes, those ILs are not liquids at room temperature and are water-soluble. These trends suggest that hydrophilic ILs generally exhibited lower eco-toxicity levels than hydrophobic ILs. However, metal extraction using hydrophilic ILs typically requires aqueous biphasic system formulation, which is not always practical. Thus, we selected IL_53 (trioctyldodecyl phosphonium nitrate, $[P_{88812}][NO_3]$), which had the highest predicted $\log EC_{50}$ value (1.91) among the hydrophobic ILs, for extraction of Nd(III). As a representative of the NA ILs, we selected IL_08 (choline glycinate, $[Cho][Gly]$), with a predicted $\log EC_{50}$ value of 4.42. Figure 3 (bottom) shows the structures of the selected ILs and their COSMO-surface views.

We selected four ILs (IL_51, IL_87, IL_53, and IL_08) for experimental examination. We purchased IL_51 from the market and synthesized the three other ILs in the laboratory. We prepared IL_87 and IL_53 via salt metathesis, and IL_08 through neutralization (Scheme 1). The Experimental Section
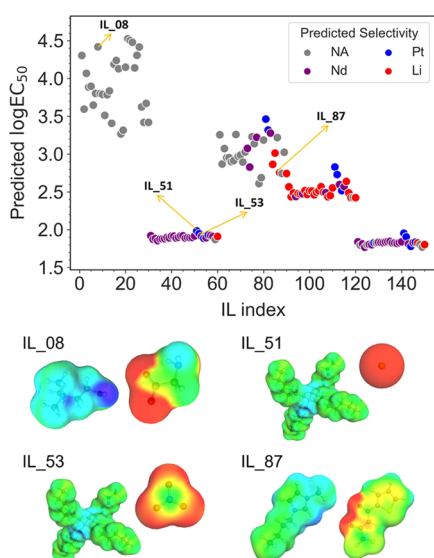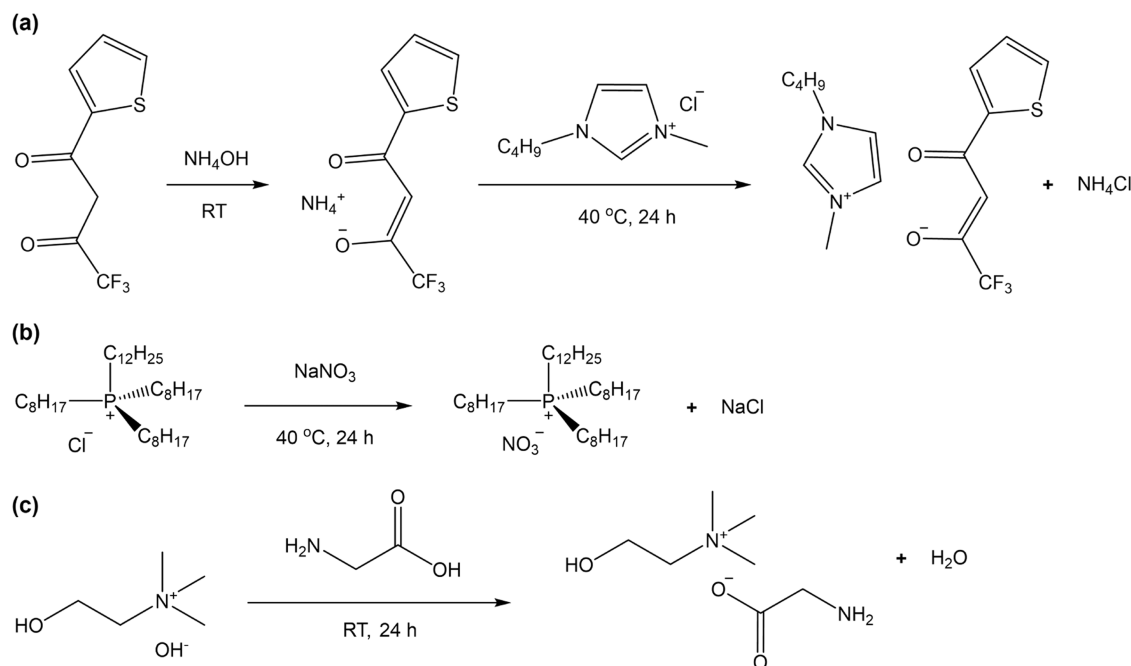
Scheme 1. Synthesis of (a) IL_87 ([Bmim][TTA]), (b) IL_53 ([P$_{88812}$][NO$_3$]), and (c) IL_08 ([Cho][Gly])

provides details of the syntheses. We confirmed the chemical structures of the synthesized ILs by proton nuclear magnetic resonance (^{1}H NMR) spectroscopy. Figures S4–S6 (Supporting Information) show the ^{1}H NMR spectra and indicate all corresponding proton peaks with minimum impurities.

We examined IL_51 for extracting Pt(IV), Li(I), and Nd(III) from 1 M HCl. We used a chloride medium to minimize ion exchange between the IL and acid. We extracted nearly 100% of the Pt(IV) to the IL phase, whereas Li(I) remained in the aqueous phase and we extracted <5% of the Nd (Figure 4a). IL_51 was a selective extractant for Pt over Li
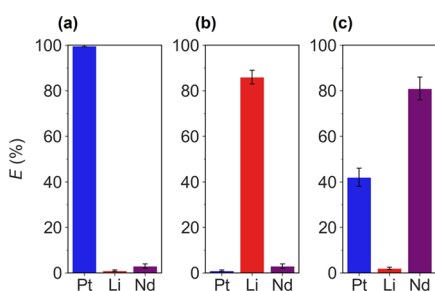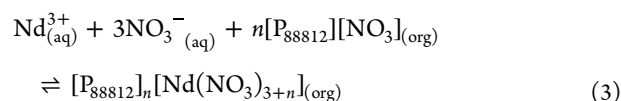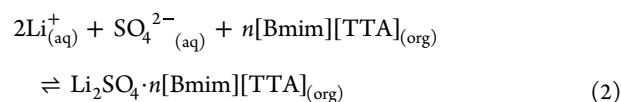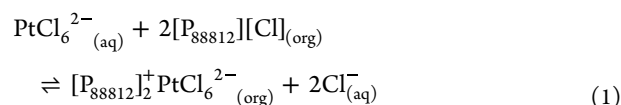

Figure 4. Extraction of Pt(IV), Li(I), and Nd(III) using (a) IL_51, (b) IL_87, and (c) IL_53.

and Nd, as predicted by the classification model. We tested IL_87 for extracting Pt(IV), Li(I), and Nd(III) from 1 M H$_2$SO$_4$. We used a sulfate medium to help suppress the partial solubility of IL_87 in water, attributable to its high salting-out effect as ranked by the Hofmeister series. We extracted ca. 85% of the Li(I) into the IL phase, whereas the extractions of Pt(IV) and Nd(III) were ca. 0 and 3%, respectively (Figure 4b). Thus, IL_87 was suitable for selective extraction of Li over Pt and Nd, in accordance with the prediction results. We used IL_53 to extract Pt(IV), Li(I), and Nd(III) from 1 M HNO$_3$. We used a nitrate medium to minimize ion exchange between the IL and acid. We extracted ca. 80% of the Nd(III)

into the IL phase, whereas the extraction of Li(I) was negligible (<3%; Figure 4c). However, we extracted approximately 40% of the Pt(IV) into the IL phase. IL_53 could be a selective extractant for Nd(III) over Li(I), but there was a competitive extraction with Pt(IV). The fact that IL_51 and IL_53 have the same cation structure might be responsible for this particular result. Nevertheless, IL_53 still has the potential to be an extractant for Nd when the coexistence of Pt in the sample is minimal. The separation factor values between Pt(IV), Li(I), and Nd(III) upon extraction using the ILs are shown in Table S4 (Supporting Information). IL_08 had a high predicted logEC$_{50}$ value, but the model classified it as NA. Apparently, the IL was unstable in acidic and basic environments. We observed precipitation after the IL contacted aqueous solutions containing HCl or NaOH (Figure S6, Supporting Information); consequently, it was unsuitable as a metal extractant. The overall assessment demonstrates the feasibility of the ML models in curating suitable ILs for selective extraction of critical metals.

$$PtCl_6^{2-}{}_{(aq)} + 2[P_{88812}][Cl]_{(org)}$$
$$\rightleftharpoons [P_{88812}]_2^+ PtCl_6^{2-}{}_{(org)} + 2Cl^-_{(aq)} \tag{1}$$

$$2Li^+_{(aq)} + SO_4^{2-}{}_{(aq)} + n[Bmim][TTA]_{(org)}$$
$$\rightleftharpoons Li_2SO_4 \cdot n[Bmim][TTA]_{(org)} \tag{2}$$

$$Nd^{3+}_{(aq)} + 3NO_3^-{}_{(aq)} + n[P_{88812}][NO_3]_{(org)}$$
$$\rightleftharpoons [P_{88812}]_n[Nd(NO_3)_{3+n}]_{(org)} \tag{3}$$

Based on knowledge from previous studies,[32–34] the metal extraction mechanisms of IL_51, IL_87, and IL_53 could be assumed to follow eqs 1–3, respectively. Pt(IV) species could be extracted via ion exchange, whereas Li(I) and Nd(III) species might be extracted via ion associations. Unfortunately, describing the mechanism in these stoichiometric equations

was not particularly helpful in understanding the nature of the extraction selectivity. Therefore, further investigations on the plausible mechanisms using slope analyses or spectroscopic techniques were not performed. Instead, we suggest using molecular dynamics simulations to scrutinize metal−IL interactions at the molecular level as future research. In addition, a more sophisticated study could be carried out in the future using deep learning algorithms. For instance, using generative neural networks, the model will be able to suggest IL structures with desired properties instead of curating ILs from numerous possibilities.

■ CONCLUSIONS

This study demonstrates a viable curation of ILs for metal extraction by ML. We prepared two ML models based on the random forest algorithm: classification and regression. We used both models to learn and predict the metal selectivity and eco-toxicity level of ILs. The classification and regression models had an accuracy score of 0.82 and an R^2 value of 0.76. The proposed models identified both cations and anions of ILs as the crucial factors that determine metal selectivity, whereas cations had a greater contribution to the eco-toxicity level. On the basis of the predictions from the ML models, we selected $[P_{88812}][Cl]$, $[Bmim][TTA]$, and $[P_{88812}][NO_3]$ for assessment in the laboratory. On the basis of the mixture solutions, we extracted (with substantial selectively) approximately 100% of Pt(IV), 85% of Li(I), and 80% of Nd(III) by each designated IL. The present study provides new insights into the design of ILs for the extraction of critical metals. Further improvements of the ML models could potentially help address various problems that are typically encountered in practical metal extraction.

■ EXPERIMENTAL SECTION

Preparation of ML Models. The learning datasets were acquired by carefully collecting them via indexing websites (such as Web of Science, Scopus, and Google Scholar) using the following keywords: (i) extraction of platinum, (ii) extraction of lithium, (iii) extraction of neodymium, and (iv) toxicity of ionic liquids. Two kinds of datasets were obtained: classification and regression. The classification dataset consisted of 76 ILs with their selectivity for Pt, Li, and Nd extraction, and ILs that were not designated for extraction of those metals were labeled as NA. In this study, selectivity is defined as the tendency of ionic liquids to extract a particular metal ion. The regression dataset contained 110 ILs with their eco-toxicity level evaluated against the marine bacterium *Aliivibrio fischeri*, represented by EC_{50} values. EC_{50} can be defined as the concentration required to obtain a 50% lethal effect on the bacterium. The higher the EC_{50} value, the lower the eco-toxicity level. We converted the EC_{50} into its logarithmic value ($\log EC_{50}$) to normalize the data scale. Each IL structure was converted into a σ-profile as the molecular descriptor using DFT and COSMO−RS calculations. Random forest classifier and random forest regressor algorithms from the scikit-learn module were selected to build the ML models.[35] Hyperparameters of the models were optimized using a grid search, and the performance was evaluated using cross-validation. The Supporting Information provides additional descriptions of the computational chemistry calculations and the ML models.

Synthesis of ILs. Four ILs were used in the experimental study: trioctyldodecyl phosphonium chloride ($[P_{88812}][Cl]$; IL_51), 1-butyl-3-methylimidazolium thenoyltrifluoroacetonate ($[Bmim][TTA]$, IL_87), trioctyldodecyl phosphonium nitrate ($[P_{88812}][NO_3]$, IL_53), and choline glycinate ($[Cho][Gly]$, IL_08). IL $[P_{88812}][Cl]$ was purchased from the market, and the three other ILs were prepared in the laboratory.

IL $[Bmim][TTA]$ was synthesized by salt metathesis (Scheme 1a). An equimolar quantity of thenoyltrifluoroacetone and ammonia (28 w/w%) were mixed in dichloromethane (DCM) at room temperature until a cloudy mixture was obtained. Subsequently, an excess of 1-butyl-3-methylimidazolium chloride (mole ratio = 1:2) was added to the mixture. The mixture was then stirred vigorously at 40 °C under reflux for 24 h. After the reaction was completed, the solution was washed with water several times to remove any unreacted reagents and byproducts. The solvent was removed with a rotary evaporator, and the final product was stored under vacuum for 2 h.

The IL $[P_{88812}][NO_3]$ was synthesized by simple ion exchange (Scheme 1b). $[P_{88812}][Cl]$ and $NaNO_3$ at a mole ratio of 1:1.2 was dissolved in methanol and stirred vigorously for 24 h at 40 °C. After the reaction was completed, the solvent was removed with a rotary evaporator. The product was then dissolved in DCM and washed with water several times to remove any unreacted reagents and byproducts. After removing DCM, the final product was stored under vacuum for 2 h.

The IL $[Cho][Gly]$ was synthesized via neutralization (Scheme 1c). An excess of glycine was dissolved in water, then choline hydroxide solution was added dropwise to the solution (mole ratio of choline:glycine = 1:1.2). The mixture was stirred for 24 h at room temperature. When the reaction was completed, the water was removed with a rotary evaporator, and the product was freeze-dried for 24 h. Subsequently, the excess glycine was removed by precipitation with a mixture of acetonitrile and methanol (9:1 v/v). The organic solvents were then removed with a rotary evaporator, and the final product was stored under vacuum for 2 h.

Solvent Extraction of Metal Ions. Aqueous phases containing 50 ppm Pt(IV), Li(I), and Nd(III) in acidic media were prepared by diluting their standard solutions in water. The acidic media for the extraction experiments using IL_51, IL_87, and IL_53 were 1 M HCl, 1 M H_2SO_4, and 1 M HNO_3, respectively. The extraction experiments were carried out by mixing each aqueous solution with the designated IL at a volume ratio of 2:1. The mixtures were agitated with a vortex mixer for 1 min before placement in a water bath shaker for 3 h at 25 °C and continuously shaken at 100 rpm. Concentrations of the metal ions in the aqueous solutions before and after extraction were monitored by inductively coupled plasma optical emission spectroscopy. The extraction efficiency (E, in percent) was calculated using eq 4, where $C_{aq}^{M,i}$ and $C_{aq}^{M,f}$ are the initial and final metal concentrations (parts per million) in the aqueous phase, respectively.

$$E = \frac{(C_{aq}^{M,i} - C_{aq}^{M,f})}{C_{aq}^{M,i}} \times 100\% \tag{4}$$

The Supporting Information provides details on the materials and instruments used in this study. No unexpected or unusually high safety hazards were encountered in the experiments.

■ ASSOCIATED CONTENT

ⓢ Supporting Information

The Supporting Information is available free of charge at https://pubs.acs.org/doi/10.1021/acssuschemeng.2c03480.

Additional descriptions of the computational chemistry calculations and the ML models, ^{1}H NMR spectra of the ILs, and details of the materials and instruments used in the experiments; All datasets and python codes used in this study were deposited at https://github.com/adroitfajar/metal-extractants (PDF)

■ AUTHOR INFORMATION

Corresponding Author

Masahiro Goto − *Department of Applied Chemistry, Graduate School of Engineering, Kyushu University, Fukuoka 819-0395, Japan;* ⓞ orcid.org/0000-0002-2008-9351; Email: m-goto@mail.cstm.kyushu-u.ac.jp

Authors

Adroit T. N. Fajar − *Department of Applied Chemistry, Graduate School of Engineering, Kyushu University, Fukuoka 819-0395, Japan*

Aditya D. Hartono − *Mathematical Modeling Laboratory, Department of Agro-Environmental Sciences, Faculty of Agriculture, Kyushu University, Fukuoka 819-0395, Japan*

Rahman Md Moshikur − *Department of Applied Chemistry, Graduate School of Engineering, Kyushu University, Fukuoka 819-0395, Japan;* orcid.org/0000-0002-0932-3741

Complete contact information is available at:
https://pubs.acs.org/10.1021/acssuschemeng.2c03480

Notes

The authors declare no competing financial interest.

■ REFERENCES

(1) IEA (International Energy Agency)*The Role of Critical Minerals in Clean Energy Transitions*, 2021.

(2) Keijer, T.; Bakker, V.; Slootweg, J. C. Circular Chemistry to Enable a Circular Economy. *Nat. Chem.* **2019**, *11*, 190−195.

(3) Laputka, M.; Xie, W. A Review of Recent Advances in Pyrometallurgical Process Measurement and Modeling, and Their Applications to Process Improvement. *Min., Metall., Explor.* **2021**, *38*, 1135−1165.

(4) Fajar, A. T. N.; Hanada, T.; Goto, M. Recovery of Platinum Group Metals from a Spent Automotive Catalyst Using Polymer Inclusion Membranes Containing an Ionic Liquid Carrier. *J. Membr. Sci.* **2021**, *629*, No. 119296.

(5) Schaeffer, N.; Vargas, S. J. R.; Passos, H.; Brandão, P.; Nogueira, H. I. S.; Svecova, L.; Papaiconomou; Coutinho, J. A. P. A HNO3-Responsive Aqueous Biphasic System for Metal Separation: Application towards CeIV Recovery. *ChemSusChem* **2021**, *14*, 3018−3026.

(6) Orefice, M.; Binnemans, K. Solvometallurgical Process for the Recovery of Rare-Earth Elements from Nd−Fe−B Magnets. *Sep. Purif. Technol.* **2021**, *258*, No. 117800.

(7) Ostermeyer, P.; Bonin, L.; Leon-Fernandez, L. F.; Dominguez-Benetton, X.; Hennebel, T.; Rabaey, K. Electrified Bioreactors: The next Power-up for Biometallurgical Wastewater Treatment. *Microb. Biotechnol.* **2022**, *15*, 755−772.

(8) Gomes, J. M.; Silva, S. S.; Reis, R. L. Biocompatible Ionic Liquids: Fundamental Behaviours and Applications. *Chem. Soc. Rev.* **2019**, *48*, 4317−4335.

(9) Cheng, J.; Deming, T. J. Synthesis, Purification and Characterization of Ionic Liquids. *Top. Curr. Chem.* **2009**, *290*, 1−40.

(10) Welton, T. Ionic Liquids: A Brief History. *Biophys. Rev.* **2018**, *10*, 691−706.

(11) Jorabchi, M. N.; Ludwig, R.; Paschek, D. Quasi-Universal Solubility Behavior of Light Gases in Imidazolium-Based Ionic Liquids with Varying Anions: A Molecular Dynamics Simulation Study. *J. Phys. Chem. B* **2021**, *125*, 1647−1659.

(12) Kim, M.; Gould, T.; Izgorodina, E. I.; Rocca, D.; Lebègue, S. Establishing the Accuracy of Density Functional Approaches for the Description of Noncovalent Interactions in Ionic Liquids. *Phys. Chem. Chem. Phys.* **2021**, *23*, 25558−25564.

(13) Chu, Y.; Zhang, X.; Hillestad, M.; He, X. Computational Prediction of Cellulose Solubilities in Ionic Liquids Based on COSMO-RS. *Fluid Phase Equilib.* **2018**, *475*, 25−36.

(14) Sivapragasam, M.; Moniruzzaman, M.; Goto, M. An Overview on the Toxicological Properties of Ionic Liquids toward Microorganisms. *Biotechnol. J.* **2020**, *15*, No. 1900073.

(15) de Almeida, A. F.; Moreira, R.; Rodrigues, T. Synthetic Organic Chemistry Driven by Artificial Intelligence. *Nat. Rev. Chem.* **2019**, *3*, 589−604.

(16) Butler, K. T.; Davies, D. W.; Cartwright, H.; Isayev, O.; Walsh, A. Machine Learning for Molecular and Materials Science. *Nature* **2018**, *559*, 547−555.

(17) Jensen, Z.; Kim, E.; Kwon, S.; Gani, T. Z. H.; Román-Leshkov, Y.; Moliner, M.; Corma, A.; Olivetti, E. A Machine Learning Approach to Zeolite Synthesis Enabled by Automatic Literature Data Extraction. *ACS Cent. Sci.* **2019**, *5*, 892−899.

(18) Jensen, Z.; Kwon, S.; Schwalbe-Koda, D.; Paris, C.; Gómez-Bombarelli, R.; Román-Leshkov, Y.; Corma, A.; Moliner, M.; Olivetti, E. A. Discovering Relationships between OSDAs and Zeolites through Data Mining and Generative Neural Networks. *ACS Cent. Sci.* **2021**, *7*, 858−867.

(19) Batra, R.; Chen, C.; Evans, T. G.; Walton, K. S.; Ramprasad, R. Prediction of Water Stability of Metal−Organic Frameworks Using Machine Learning. *Nat. Mach. Intell.* **2020**, *2*, 704−710.

(20) Jorner, K.; Tomberg, A.; Bauer, C.; Sköld, C.; Norrby, P.-O. Organic Reactivity from Mechanism to Machine Learning. *Nat. Rev. Chem.* **2021**, *5*, 240−255.

(21) Wang, G.; Fearn, T.; Wang, T.; Choy, K. L. Machine-Learning Approach for Predicting the Discharging Capacities of Doped Lithium Nickel-Cobalt-Manganese Cathode Materials in Li-Ion Batteries. *ACS Cent. Sci.* **2021**, *7*, 1551−1560.

(22) Klamt, A. Conductor-like Screening Model for Real Solvents: A New Approach to the Quantitative Calculation of Solvation Phenomena. *J. Phys. Chem. A* **1995**, *99*, 2224−2235.

(23) Zhao, X.; Wu, H.; Duan, M.; Hao, X.; Yang, Q.; Zhang, Q.; Huang, X. Liquid-Liquid Extraction of Lithium from Aqueous Solution Using Novel Ionic Liquid Extractants via COSMO-RS and Experiments. *Fluid Phase Equilib.* **2018**, *459*, 129−137.

(24) Foong, C. Y.; Mohd Zulkifli, M. F.; Wirzal, M. D. H.; Bustam, M. A.; Nor, L. H. M.; Saad, M. S.; Abd Halim, N. S. COSMO-RS Prediction and Experimental Investigation of Amino Acid Ionic Liquid-Based Deep Eutectic Solvents for Copper Removal. *J. Mol. Liq.* **2021**, *333*, No. 115884.

(25) Villarroel, E.; Olea, F.; Araya-López, C.; Gajardo, J.; Merlet, G.; Cabezas, R.; Romero, J.; Quijada-Maldonado, E. Diluent Effects in the Solvent Extraction of Rhenium (VII) with Amine Extractants in [Tf2N]-Based Ionic Liquids: Experimental and COSMO-RS Analysis. *J. Mol. Liq.* **2022**, *346*, No. 117091.

(26) Gharehdaghi, T.; Karimi-Sabet, J.; Ghoreishi, S. M.; Motallebipour, M.; Sadjadi, S. Theoretical and Experimental Study of Calcium Extraction Using Ionic Liquids: COSMO-RS Approach. *J. Mol. Liq.* **2022**, *345*, No. 118174.

(27) Koutsoukos, S.; Philippi, F.; Malaret, F.; Welton, T. A Review on Machine Learning Algorithms for the Ionic Liquid Chemical Space. *Chem. Sci.* **2021**, *12*, 6820−6843.

(28) Géron, A. *Hands-on Machine Learning with Scikit-Learn, Keras, and TensorFlow*; O'Reilly Media, 2019.

(29) Izadiyan, P.; Fatemi, M. H.; Izadiyan, M. Elicitation of the Most Important Structural Properties of Ionic Liquids Affecting Ecotoxicity in Limnic Green Algae; a QSAR Approach. *Ecotoxicol. Environ. Saf.* **2013**, *87*, 42−48.

(30) Peric, B.; Sierra, J.; Martí, E.; Cruañas, R.; Garau, M. A. Quantitative Structure-Activity Relationship (QSAR) Prediction of (Eco)Toxicity of Short Aliphatic Protic Ionic Liquids. *Ecotoxicol. Environ. Saf.* **2015**, *115*, 257−262.

(31) Passino, D. R. M.; Smith, S. B. Acute Bioassays and Hazard Evaluation of Representative Contaminants Detected in Great Lakes Fish. *Environ. Toxicol. Chem.* **1987**, *6*, 901−907.

(32) Firmansyah, M. L.; Kubota, F.; Yoshida, W.; Goto, M. Application of a Novel Phosphonium-Based Ionic Liquid to the Separation of Platinum Group Metals from Automobile Catalyst Leach Liquor. *Ind. Eng. Chem. Res.* **2019**, *58*, 3845−3852.

(33) Cai, C.; Hanada, T.; Fajar, A. T. N.; Goto, M. An Ionic Liquid Extractant Dissolved in an Ionic Liquid Diluent for Selective Extraction of Li(I) from Salt Lakes. *Desalination* **2021**, *509*, No. 115073.

(34) Rout, A.; Binnemans, K. Solvent Extraction of Neodymium(III) by Functionalized Ionic Liquid Trioctylmethylammonium Dioctyl Diglycolamate in Fluorine-Free Ionic Liquid Diluent. *Ind. Eng. Chem. Res.* **2014**, *53*, 6500−6508.

(35) Pedregosa, F.; Varoquaux, G.; Gramfort, A.; Michel, V.; Thirion, B.; Grisel, O.; Blondel, M.; Prettenhofer, P.; Weiss, R.; Dubourg, V.; et al. Scikit-Learn: Machine Learning in Python. *J. Mach. Learn. Res.* **2011**, *12*, 2825−2830.